COMMUNICATION

Nanowire-Induced Wurtzite InAs Thin Film on Zinc-Blende InAs Substrate

By *Jiming Bao, David C. Bell, Federico Capasso, Natasha Erdman, Dongguang Wei, Linus Fröberg, Thomas Mårtensson,* and *Lars Samuelson**

Synthesis of materials with a desired crystal structure is a major challenge in materials engineering. Single-crystal thin films grown by epitaxy typically adopt the same crystal structure as that of their substrates. Here, we report on the observation of a wurtzite InAs thin-film structure on a zinc-blende InAs substrate. Electron-backscatter diffraction (EBSD) and transmission electron microscopy (TEM) confirm the wurtzite crystal structure. The bandgap of wurtzite InAs, obtained by low-temperature photoluminescence, is found to be 20% higher than that of zinc-blende InAs, in good agreement with band-structure calculations.[1,2] Microscopy studies suggest that the wurtzite InAs thin film is the result of step flow along the surface from the base of wurtzite InAs nanowires synthesized by chemical beam epitaxy on a zinc-blende InAs substrate,[3] leading to layer-by-layer lateral expansion. Although the conditions for the controlled growth of wurtzite InAs films need to be investigated, our observations suggest a new approach to creating thin films with nanowire-induced crystal structure. The creation and integration of a material with different crystal structures, such as polymorphism and the associated heterocrystalline heterostructures, could open up new opportunities in bandgap engineering and related device applications.[2,4–8]

[*] Prof. L. Samuelson, Dr. L. Fröberg, Dr. T. Mårtensson
Solid State Physics, Lund University
PO Box 118, 22100 Lund (Sweden)
E-mail: lars.samuelson@ftf.lth.se
Prof. J. M. Bao
Department of Electrical and Computer Engineering
University of Houston
Houston, TX 77204 (USA)
Dr. D. C. Bell, Prof. F. Capasso
School of Engineering and Applied Sciences
Harvard University
Cambridge, MA 02138 (USA)
Dr. D. C. Bell
Center for Nanoscale Systems
Harvard University
Cambridge, MA 02138 (USA)
Dr. N. Erdman
JEOL USA,
11 Dearborn Road
Peabody, MA 01960 (USA)
Dr. D. Wei
Carl Zeiss SMT, Inc.
One Corporation Way
Peabody, MA 01960 (USA)

DOI: 10.1002/adma.200900617

Polymorphism or polytypism has been a fascinating subject because materials with different crystal structures can exhibit very distinct electronic and optical properties, although they are chemically identical.[4,5] Typically, there is only one stable structure for a bulk material under ambient condition, and the synthesis and preservation of a crystal with a different structure require high pressure and extreme temperatures.[9,10] It has been observed that size and dimensionality can have a strong impact on the crystal structure of a material.[3,11–15] For example, III–V (except for nitrides) and group IV bulk semiconductors naturally take zinc-blende or diamond structure, respectively, but chemically synthesized whiskers or nanowires often exhibit a wurtzite structure.[3,11–15] Recent advances in nanowire synthesis have achieved controlled growth of single-crystal wurtzite nanowires, single-crystal zinc-blende nanowires, as well as nanowires with periodically alternating structures between wurtzite and zinc-blende.[13–17] Despite alternative crystal structures generated in nanowires, materials in the form of single-crystal thin film or two-dimensional structures are still desirable in many applications, due to their ease of device fabrication and integration. However, it is a challenge to grow thin films with a structure different from that of the bulk substrate, because single-crystal thin films obtained by epitaxial growth, such as molecular beam epitaxy or chemical vapor deposition, usually have the same crystal structure as the substrate.

InAs is a semiconductor with high electron mobility related to its low bandgap. As such, InAs, especially in nanostructures such as quantum dots and nanowires, is being explored for applications in optoelectronic and high-speed electronic devices.[18–23] Like other III–V nanowires, InAs nanowires frequently exhibit wurtzite crystal structures.[3,11,21–23] Experimental studies of these wurtzite structures, as well as theory, have indicated that the wurtzite InAs has a higher bandgap than zinc-blende InAs.[1,2,24–26] This indirect experimental evidence includes photoluminescence of InAs/InP core/shell nanowires,[24] the g factor of InAs nanowire quantum dots in InP nanowires,[25] and photocurrent measurements of InAsP nanowires.[26] However a direct measurement of the bandgap of wurtzite InAs has not yet been reported.

Figure 1 shows scanning electron microscopy (SEM) images of the sample. The InAs nanowires grow vertically from the substrate. Due to the conditions for the formation of the nanowires, the wurtzite crystal structure is preferred, in contrast to the zinc-blende crystal structure that is energetically favorable for bulk InAs.[3,11,12,21–26] As part of the nanowire fabrication process, a pyramid-like base forms at the root of each InAs nanowire. Broader-area platelets form between the pyramid

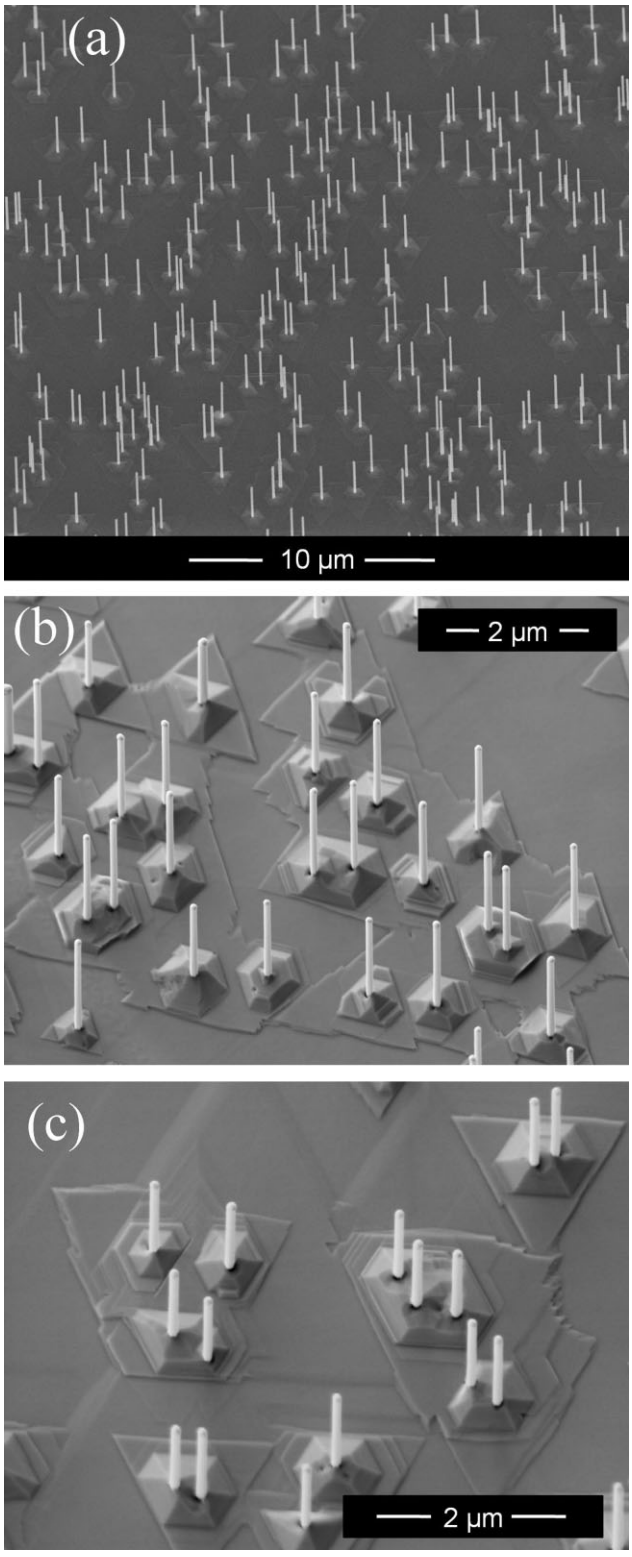

Figure 1. SEM images of the InAs sample grown on a InAs substrate at increasing magnification. The hexagonal pyramids and small platelets right beneath the pyramids are clearly seen at the bottom of nanowires. It can also be seen from b) and especially from c) that beneath isolated platelets there are large-size overgrown layers that connect nanowires and cover the entire top surface.

nanowires bases. These platelets have been observed in several areas of the sample to fill the available surface space.

EBSD was performed using a JSM-7001F, which was used to probe the crystal structure of the top surface layers of the samples. Figures 2 and 3 show the EBSD patterns at electron energies of 20 keV and 5 keV, respectively. The analysis was carried out at an incident angle of 70° with beam diameters of approximately 2.5 and 4 nm at 20 and 5 keV, respectively. Results from electron flight simulator show that 20 keV electrons have a sample interaction volume that extends to a penetration depth of 600 nm, while the 5 keV electrons have a smaller interaction volume, and are more sensitive to the top 100 nm layer materials.

The 20 keV EBSD patterns in Figure 2 indicate that the bases of InAs nanowires, that is, pyramids, have a wurtzite structure. These patterns also indicate that the pyramids are thicker than 600 nm, as the EBSD pattern from zinc-blende substrate is not visible. The EBSD pattern from the flat regions between nanowires is dominated by the zinc-blende phase of the InAs substrate. In contrast, the 5 keV EBSD pattern (Fig. 3) from a similar flat region shows a mixture of EBSD wurtzite and zinc-blende patterns. We conclude that there must be a top wurtzite thin-film structure that has a thickness $\leq$100 nm. In summary, from the combined EBSD patterns at the two energies, we conclude that the surface of the zinc-blende InAs substrate, even in the flat regions, is covered by a wurtzite InAs phase.

In order to directly image the thickness and structure of the top layer, we prepared transmission electron microscopy (TEM) cross-section samples (10 μm × 15 μm). The low-resolution TEM cross-section image in Figure 4 clearly shows that there is a layer on top of the substrate that is between 20 nm to 40 nm thick. This serves only as an estimate, given that the TEM image samples represent a very small fraction of the surface layer. The high-resolution TEM image in Figure 5 shows an abrupt interface between substrate and top layer. The top layer and pyramid show a wurtzite lattice structure.

Photoluminescence (PL) measurements were employed to probe the electronic and optical properties of the top wurtzite InAs layer. Figure 6 shows a typical PL spectrum excited by an 808 nm CW laser. The spectrum remains the same when a shorter-wavelength, 514 nm, laser is used, as also shown in the figure. The spectrum from the InAs sample with the overgrown wurtzite structure shows a peak at 0.52 eV, in contrast to the spectrum from a clean InAs substrate that is centered at the zinc-blende InAs bandgap of 0.41 eV.[27,28] The observed 0.52 eV is assigned to the bandgap of wurtzite InAs. This value is slightly higher than the value from theoretical calculations,[1,2] but agrees well with the value extrapolated from the measurement of InAsP nanowires and InAs/InP core/shell nanowires.[24,26]

It is to be noted that the wurtzite InAs PL comes from wurtzite pyramids and platelets, not from wurtzite InAs nanowires. This observation is based on the following control experiments. First, we measured the PL of the sample before and after removing of InAs nanowires. We found that there is no change in the PL spectra. This result indicates that PL from wurtzite nanowires is too weak to be measured. Second, we measured PL of InAs nanowires transferred to a clean silicon substrate. The transfer was performed in such a way that the number of photoexcited InAs nanowires on silicon substrate is about the same as on the original InAs substrate. No measurable luminescence was

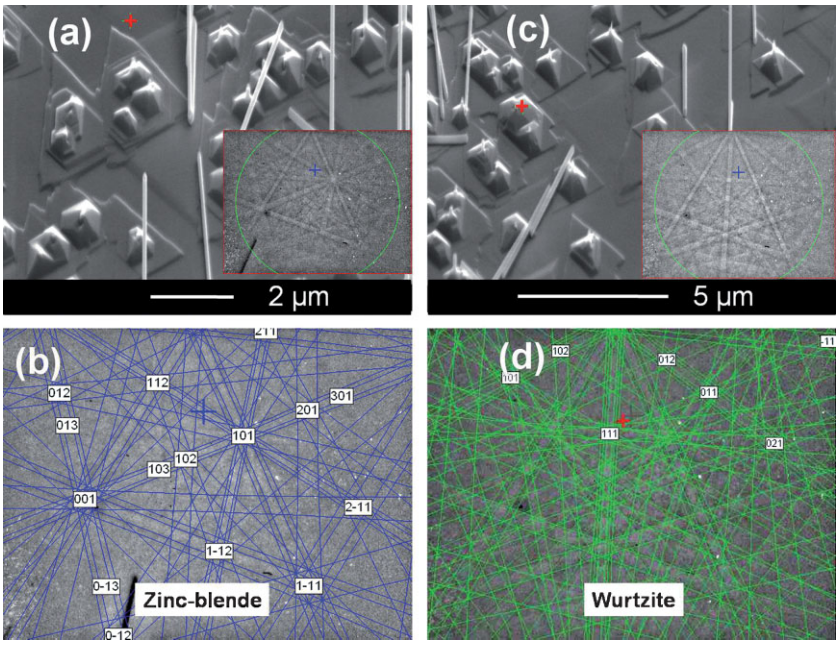

Figure 2. EBSD patterns from different spots on the sample surface. The accelerating voltage is 20 kV, corresponding to a 600 nm electron penetration depth. a) Diffraction pattern (inset) from a flat region marked by a red cross. b) The indexed pattern of (a) reveals a zinc-blende crystal structure. c) Diffraction pattern (inset) from a pyramid indicated by a red cross. d) The indexed pattern of (c) indicates that the pyramid has a wurtzite crystal structure.

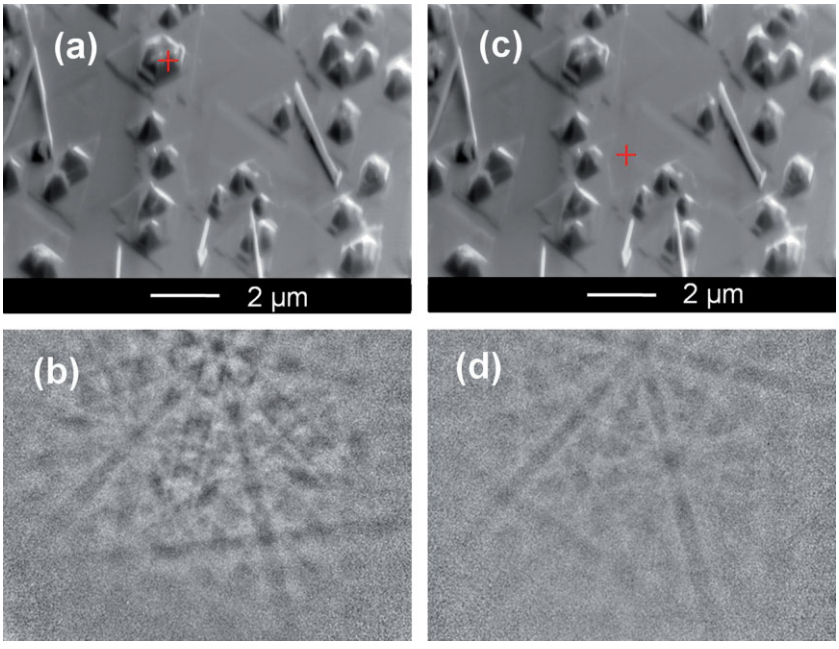

Figure 3. EBSD patterns from different spots on the sample surface. The accelerating voltage is 5 kV, corresponding to a 100 nm penetration depth. (Left) Diffraction pattern (b) from a pyramid marked by a red cross in a). The pattern shows a wurtzite crystal structure. (Right) Diffraction pattern (d) from a flat platelet region marked by a red cross in c). The pattern is a mixture of wurtzite and zinc-blende structures.

detected from wurtzite InAs nanowires. As a matter of fact, we are not aware of any reports on PL from pure wurtzite InAs nanowires in the literature. The absence of InAs PL is likely due to a high surface recombination.

We also moved the laser spot (≈200 μm in diameter) across the whole surface of the sample (note that micro-PL cannot be implemented in the mid-IR in our setup, as it would require collection with the same objective used to focus the short wavelength pump laser); no noticeable variation in PL was observed, and a PL peak corresponding to the bandgap of the zinc-blende InAs substrate was not observed until the top layer was mechanically polished away. In the following, we provide a plausible scenario of how this can occur. Band-structure calculations have shown that interfaces between wurtzite and zinc-blende crystal structures of the same III–V semiconductor form staggered (known also as type II) heterojunctions.[2] Recent PL data in InP nanowires with random wurtzite-zinc-blende superlattices due to twinning could only be explained by such a band line-up.[8] This type of heterojunction, by its very nature, promotes spatial separation of electrons and holes. While photogenerated carriers generated near the surface will partially recombine in the wurtzite InAs surface layer, giving rise to a PL signal at the wurtzite bandgap, the majority of electrons and holes generated in the InAs substrate are instead spatially separated, because they are created near the interface due to the very short absorption length in InAs for laser at 514 nm and 808 nm, corresponding to an absorption length of ≈25 nm and ≈130 nm, respectively.[29] The net effect is quenching of the PL at the zinc-blende bandgap.

The shape of the PL spectrum, which arises from the recombination of electrons with optically generated holes, is indicative of the well-known Fermi level pinning in the conduction band of surface InAs, with the Fermi-edge singularity playing a role in the enhancement of the PL signal on the high-energy side of the spectrum.[28] But additional factors will contribute to the width and shape of the spectrum: i) the fact that it is collected from a large area with significant spatial inhomogeneity in the InAs crystal structure, ii) the presence of band tails associated with defects, and iii) the imperfections of the wurtzite structure, mainly stacking faults. In fact, the PL intensity is much smaller than in the InAs zinc-blende substrate case, indicative of a large nonradiative recombination rate.

Note from the SEM pictures that the surface has a hierarchical structure: from pyramids

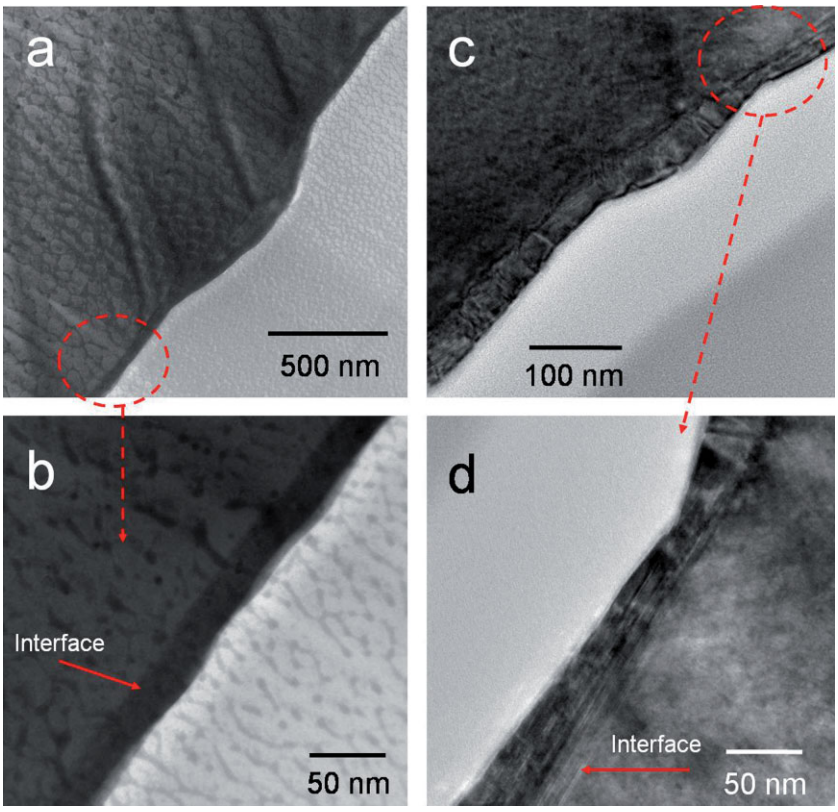

Figure 4. Cross-section TEM images from two samples prepared by FIB. Bright areas are amorphous carbon deposited to protect the top wurtzite layer during FIB milling. A top layer on the substrate about 20 nm to 40 nm thick can be seen in both samples. Also seen are grains and damage due to ion milling and Ga redeposition.

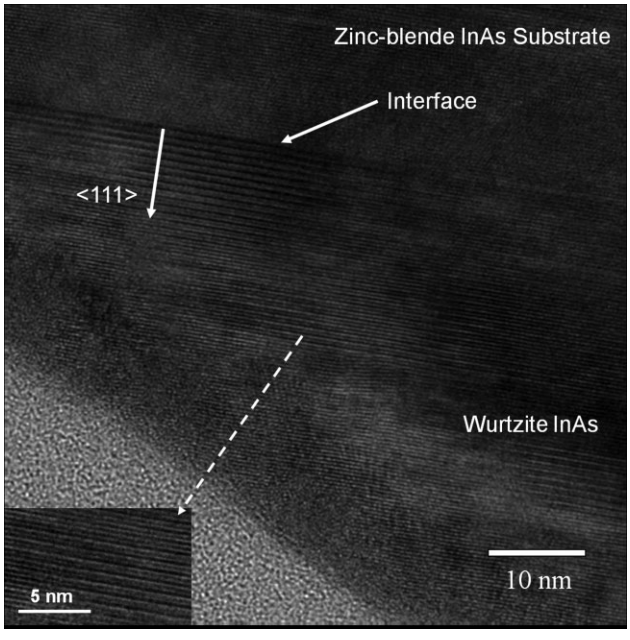

Figure 5. High-resolution TEM images from the interface between the zinc-blende InAs substrate and the top wurtzite layer, as indicated by the EBSD patterns near a pyramid. The normal to the surface is the ⟨111⟩ direction. There is a clear transition of the crystal lattice structure from zinc-blende to wurtzite.

bases, to small plateaus (with a thickness on the order of 100 nm), to large plateaus with a thickness that is hard to determine from SEM. The surface is never perfectly flat, even on big plateaus. As a result, one can say that approximately 50% of the top surface is covered by optically thick wurtzite InAs structures. The TEMs of Figure 4c and d might indicate the thinnest part of surface where two plateaus meet.

These observations lead us to the conclusion that there is an optically thick wurtzite layer covering the majority of the InAs substrate. Because Figure 6 shows that the PL peak intensity at 0.41 eV from a clean InAs substrate is stronger than the peak intensity at 0.52 eV from wurtzite layer, if there were any regions not covered by a wurtzite layer in the sample with grown nanowires, a PL signal peaked at the bandgap of the zinc-blende InAs substrate would be observed.

An understanding of how the surface layer is formed can intuitively be achieved by noting that the pyramidal segment at the base of each nanowire (Fig. 1) is a source of step flow growth along the surface., leading to layer-by-layer lateral expansion that preserves the stacking sequence (wurtzite) of the wire. The stacking sequence of the nanowire itself is governed by growth parameters,[30] and is wurtzite under the used conditions. Thus, the nanowire provides a seeding point of controlled crystal structure, independent of the stacking sequence of the substrate (ZB or WZ).

In summary, based on EBSD, TEM, and PL measurements, we can conclude that besides visible wurtzite pyramids and nanowires shown in Figure 1, there is a 2D wurtzite InAs structure covering the surface of the InAs substrate. They adopt the crystal structure of the nanowire, which is wurtzite, thus

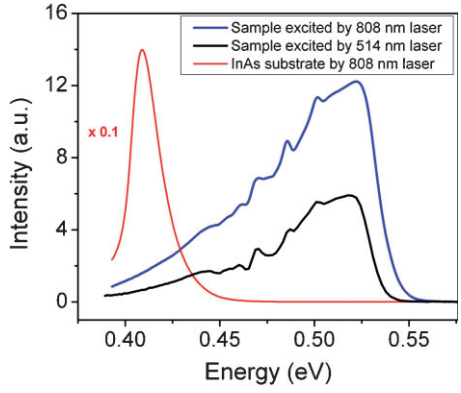

Figure 6. Photoluminescence spectra of the InAs nanowire sample (blue and black) and a clean InAs reference substrate (red). The measurements were performed at 7 K. The spectrum in black was obtained using 514 nm Ar line as excitation source, while the other two spectra (in red and blue) were excited by a 808 nm laser at the same intensity.

creating 2D-like InAs in the wurtzite crystal structure. We obtained a bandgap of 0.52 eV for wurtzite InAs at low temperature, in good agreement with theory. The 2D-like structures are composed of large-area platelets. Future work will concentrate on the detailed understanding and control of the nanowire-induced growth mechanism, which could be used to synthesize other wurtzite thin films not obtainable by using conventional epitaxial techniques.

Experimental

The growth of wurtzite InAs structures was performed in a chemical beam epitaxy system on InAs(111)B substrates [3]. No cleaning of the substrates was performed prior to growth. The nucleation and growth of nanowires on the substrate is assisted by Au aerosol particles deposited ex situ. The substrate was annealed at 520 °C for 15 min under As pressure to remove the native oxide, followed by growth at 420 °C using tertiarybutylarsine (TBAs) and trimethylindium (TMIn) as precursors. TBAs were thermally cracked upon entering the growth chamber, whereas TMIn was sent in as-is, and decomposes on the substrate surface.

The TEM samples were cut from the sample in Figure 1 using focused ion beam (FIB) milling. The final polish of the TEM samples was with low-energy Ar ion milling.

Low-temperature PL was performed in an optical cryostat equipped with a CaF_2 window that is optically transparent out to $\lambda = 5$ μm. Continuous Wave (CW) lasers were used to photoexcite the sample. A liquid-nitrogen-cooled InSb photodetector was used to measure luminescence from the sample.

Acknowledgements

The authors thank P. Kirby for assistance in the preparation of TEM samples, D. Lange for the XPS measurements. Partial financial support from the National Science Foundation Nanoscale Science and Engineerings Center at Harvard is gratefully acknowledged. The support from the Center for Nanoscale Systems (CNS) at Harvard University is also gratefully acknowledged. Harvard CNS is a member of the National Nanotechnology Infrastructure Network (NNIN). This work was carried out within the Nanometer Structure Consortium in Lund and was supported by the Swedish Foundation for Strategic Research (SSF), the Swedish Research Council (VR), the European Community (EU contract no. 015783 NODE) and the Knut and Alice Wallenberg Foundation (KAW).

Received: February 20, 2009
Revised: May 10, 2009
Published online: July 2, 2009

[1] Z. Zanolli, F. Fuchs, J. Furthmueller, U. von Barth, F. Bechstedt, *Phys. Rev. B* **2007**, *75*, 245121.
[2] M. Murayama, T. Nakayama, *Phys. Rev. B* **1994**, *49*, 4710.
[3] B. J. Ohlsson, M. T. Björk, A. I. Persson, C. Thelander, L. R. Wallenberg, M. H. Magnusson, K. Deppert, L. Samuelson, *Phys. E* **2002**, *13*, 1126.
[4] G. C. Trigunayat, *Solid State Ionics* **1991**, *48*, 3.
[5] C. Y. Yeh, Z. W. Lu, S. Froyen, A. Zunger, *Phys. Rev. B* **1992**, *46*, 10086.
[6] S. Y. Ren, J. D. Dow, *Phys. Rev. B* **1989**, *39*, 7796.
[7] Z. Z. Bandic, Z. Ikonic, *Phys. Rev. B* **1995**, *51*, 9806.
[8] J. M. Bao, D. C. Bell, F. Capasso, J. B. Wagner, T. Mårtensson, J. Trägårdh, L. Samuelson, *Nano Lett.* **2008**, *8*, 836.
[9] R. H. Wentorf, J. S. Kasper, *Science* **1963**, *139*, 338.
[10] M. I. McMahon, R. J. Nelmes, *Phys. Rev. Lett.* **2005**, *95*, 215505.
[11] K. Takahashi, T. Moriizumi, *Jpn. J. Appl. Phys.* **1966**, *5*, 657.
[12] B. Mandl, J. Stangl, T. Mårtensson, A. Mikkelsen, J. Eriksson, L. S. Karlsson, G. Bauer, L. Samuelson, W. Seifert, *Nano Lett.* **2006**, *6*, 1817.
[13] A. F. Morral, J. Arbiol, J. D. Prades, A. Cirera, J. R. Morante, *Adv. Mater.* **2007**, *19*, 1347.
[14] M. Mattila, T. Hakkarainen, M. Mulot, H. Lipsanen, *Nanotechnology* **2006**, *17*, 1580.
[15] P. Mohan, J. Motohisa, T. Fukui, *Nanotechnology* **2005**, *16*, 2903.
[16] R. E. Algra, M. A. Verheijen, M. T. Borgström, L. F. Feiner, G. Immink, W. J. P. van Enckevort, E. Vlieg, E. P. A. M. Bakkers, *Nature* **2008**, *456*, 369.
[17] Q. H. Xiong, J. Wang, P. C. Eklund, *Nano Lett.* **2006**, *6*, 2736.
[18] H. Saito, K. Nishi, S. Source, *Appl. Phys. Lett.* **2001**, *78*, 267.
[19] N. Sarukura, H. Ohtake, S. Izumida, Z. Liu, *J. Appl. Phys.* **1998**, *84*, 654.
[20] P. Gu, M. Tani, S. Kono, K. Sakai, X. C. Zhang, *J. Appl. Phys.* **2002**, *91*, 5533.
[21] H. Pettersson, J. Trägårdh, A. I. Persson, L. Landin, D. Hessman, L. Samuelson, *Nano Lett.* **2006**, *6*, 229.
[22] E. Lind, A. I. Persson, L. Samuelson, L. E. Wernersson, *Nano Lett.* **2006**, *6*, 1842.
[23] A. I. Persson, M. T. Bjork, S. Jeppesen, J. B. Wagner, L. R. Wallenberg, L. Samuelson, *Nano Lett.* **2006**, *6*, 403.
[24] Z. Zanolli, L. E. Fröberg, M. T. Björk, M. E. Pistol, L. Samuelson, *Thin Solid Films* **2006**, *515*, 793.
[25] M. T. Björk, A. Fuhrer, A. E. Hansen, M. W. Larsson, L. E. Fröberg, L. Samuelson, *Phys. Rev. B* **2005**, *72*, 201307.
[26] J. Trägårdh, A. I. Persson, J. B. Wagner, D. Hessman, L. Samuelson, *J. Appl. Phys.* **2007**, *101*, 123701.
[27] Z. M. Fang, K. Y. Ma, D. H. Jaw, R. M. Cohen, G. B. Stringfellow, *J. Appl. Phys.* **1990**, *67*, 7035.
[28] F. Fuchs, K. Kheng, P. Koidl, K. Schwarz, *Phys. Rev. B* **1993**, *48*, 7884.
[29] A. B. Djurisic, A. D. Rakic, P. Kwok, E. H. Li, M. L. Majewski, *J. Appl. Phys.* **1999**, *85*, 3638.
[30] P. Caroff, K. A. Dick, J. Johansson, M. E. Messing, K. Deppert, L. Samuelson, *Nat. Nanotechnol.* **2009**, *4*, 50.